CHEMISTRY
A European Journal

A Journal of
ChemPubSoc Europe

Accepted Article

Title: Supermacrocyclic assemblies by Hydrogen-Bond Codes of C7-Phenol Pyrazolo and Pyrrolo Derivatives of Adenine

Authors: Yingying Chai, Xinglong Zhou, Changfu Li, Beibei Ma, Zhen Shen, Ridong Huang, Hai Chen, Bojiang Chen, Weimin Li, and Yang He

To be cited as: *Chem. Eur. J.* 10.1002/chem.201803429

Link to VoR: http://dx.doi.org/10.1002/chem.201803429

Supported by
ACES

WILEY-VCH

10.1002/chem.201803429

WILEY-VCH

Supermacrocyclic assemblies by Hydrogen-Bond Codes of C7-Phenol Pyrazolo and Pyrrolo Derivatives of Adenine

Yingying Chai,[a,c,#] Xinglong Zhou,[b,#] Changfu Li,[a,c] Beibei Ma,[a] Zhen Shen,[a] Ridong Huang,[a] Hai Chen,[a] Bojiang Chen,[a] Weimin Li*[a] and Yang He*[a]

Abstract: Hydrogen bond (HB) mediated base pair motifs are versatile scaffolds of diverse supramolecular constructs. Here, we report that two novel four and six-membered supermacrocyclic assemblies with intriguing geometries can be self-assembled from two new adenine derivatives, APN (**1**) and APC (**2**). The conversion of a conventional HB acceptor, N8 of **1**, to a non-conventional HB donor, C8-H of **2**, has a pronounced impact on the whole intricate overall HB network and self-assembly patterns, epitomizing the subtleties in design and exploitation of such base pair motifs as promising tectons for building supramolecular architectures.

Macrocycles have been attractive entities in the physical, chemical, material and biological sciences.[1] Paralleling their covalent counterparts, supramolecular macrocycles have been drawing increasing interest for their innate adaptivity.[2] HB information-bearing nucleobases have been judiciously utilized to build programmable supramolecular cyclic structures, from trimeric to hexametric macrocycles.[3-6] Importantly, the HB pattern alone in these cases is insufficient to univocally govern the outcome of the assembly, and the formation of these cyclic arrays also depends on additional metal ion binding or steric effects. Pure HB motifs based supermacryocyclic assemblies were achieved by Lehn and Fenniri, et al, through the construction of rosette structures via Janus-type GC base derivatives.[7,8] Inspired by these works, we designed and synthesized a series of Janus-type nucleosides by merging all four chemical letters of the genetic alphabet into the fused pyrimido[4,5-d]pyrimidine heterocyclic system. However, our attempt to build hexameric supermacrocyclic assemblies based on six-membered Watson-Crick base pairing motif from the bidentate J-AT series was unsuccessful.[9-11]

This prompted us to investigate other adenine analogues in the pyrazolo[3,4-d]pyrimidine and pyrrolo[2,3-d]pyrimidine contexts.[12] We have found two new adenine derivatives, hereby refered to as APN (**1**, A for adenine, P for phenol, N for N8) and APC (**2**, C for C8), bearing phenol and *tert*-butyl groups at C7 and N9 positions (Figure 1a), can form supramolecular ring structures with different base pair motifs, sizes, shapes and assembling patterns. Herein, the fine details and properties of these supermacrocyclic assemblies and how subtle structural parameter alter these novel supramolecular cycles through different HB codes are described.

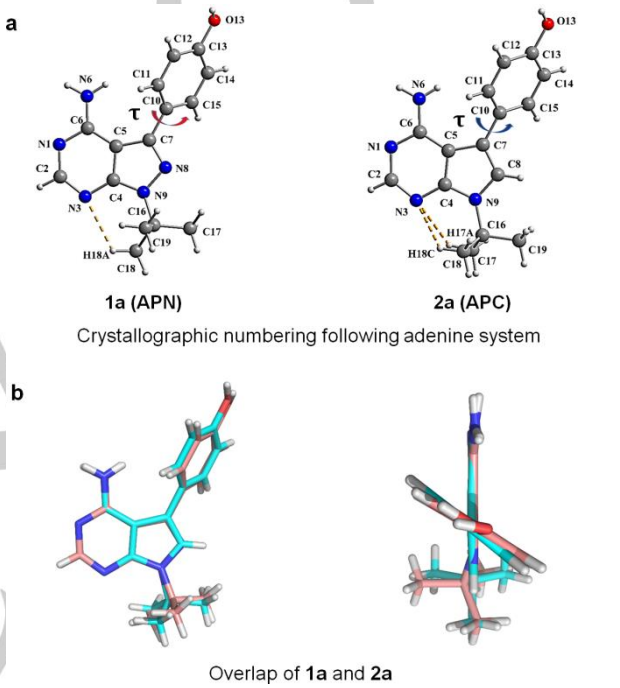

Figure 1. a): The ball-stick representations of conformers **1a** and **2a**. b): The overlap graphs of **1a** and **2a** from side-views (up) and top-views (down).

Due to steric hindrance from the *tert*-butyl group, two linear synthetic routes were adopted. For **1**, the key pyrazole precursor **8** was obtained following reported procedures.[13] For **2**, the pyrrolopyrimidine nucleus **11** was obtained by cyclization from a dichloropyrimidine precursor.[14] The 7-phenol group was introduced via Suzuki−Miyaura cross coupling with either bromine or iodine derivatives (Scheme S1, S2). Suitable single crystals for X-ray diffraction analysis were obtained from MeOH/H_2O (10:1) for **1**, with a triclinic P-1 space group, and from MeOH/CH_2Cl_2 (2:1) for **2**, with a trigonal R-3 space group.

At the monomeric molecular level, a pair of conformational enantiomers exists in the single crystals of both **1** and **2**. Using the torsion angle τ (C5-C7-C10-C11), we denote the conformers as **1a** (τ = 60.04)/**1b** (τ = -60.04), and **2a** (τ = 51.72)/ **2b** (τ = -51.72) (Figure 1b, S1). Within the unit cell of **1**, only two inversion related conformational enantiomers are present. In contrast, a total of 18 conformers of **2** are located within the unit cell, leading to a much larger unit-cell and a high Z'=3. From the overlap graphs, the molecular shapes of the corresponding conformers of the two series are found to be almost the same (Figure 1b, S1). The electron densities of the Watson-Crick

[a] Y Chai, C Li, B Ma, Z Shen, R Huang, H Chen, B Chen, W Li and Y He
Precision Medicine Research center, Department of Respiratory and Critical Care Medicine, West China Hospital, Sichuan University, Chengdu, Sichuan 610041, China
E-mail: heyangqx@scu.edu.cn (Yang He)
[b] X Zhou
School of Chemical Engineering, Sichuan University
Chengdu, Sichuan, 610041, China
[c] Y Chai, C Li
Institute for Nanobiomedical Technology and Membrane Biology, Sichuan University
Chengdu, Sichuan, 610041, China
# These authors contributed equally to this study

Supporting information for this article is available on the WWW under http://dx.doi.org/10.1002/chem.2018xxxxx.

10.1002/chem.201803429

edges (N1 and 6-NH_2) and the N3 atoms on the adenine-pyrimidine rings do not differ much between these two systems and the electron density differences reside on the pyrazolo and pyrrolo rings (*ab initio* 6-31G* level, Figure S2). The UV absorption spectra are displayed in Figure S3.

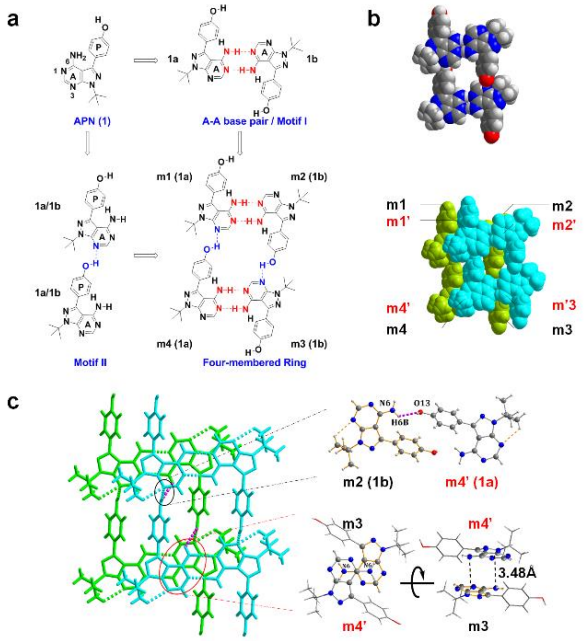

Figure 2. a): The HB motifs I, II and the four-membered ring. b): The space-filling views of four-membered ring and their cross-layered spatial arrangement. c): The intermolecular interactions of the two neighboring crossed-layered rings: HB between 6-NH_2 and phenol-OH, upper-right and amino-aromatic type π-π interactions, lower-right.

At the single crystal level of **1**, an adenine-adenine (A-A) base pair connecting opposite conformational enantiomers via the Watson-Crick edges (N1 and 6-NH_2) is disclosed (motif I). Meanwhile, another intermolecular HB motif (motif II, Figure 2a) is also formed between the N3 and the phenol group of the same conformational enantiomers. Together, a novel four-membered adenine analog-based ring structure is formed by these two HB motifs (Figure 2a). Considering these individual four-membered rings separately, there are empty rectangular holes (6.04 × 6.52 $Å^2$, Figure S4) encircled by four interconnected molecules, m1-m4 (Figure 2b). These rings form ladder-like ribbons extending along the phenol-N3 direction, and ladders on the same plane layers are in turn associated together through the interdigital *tert*-butyl side-chains (Figure S5). Considering the situation across different layers, the four-membered rings in neighbouring layers are connected by additional HBs and amino-aromatic type π-π interactions (Figure 2c). Thus, APN actually forms a closely packed crystal structure with the four-membered rings embedded in interlinked ladder-like ribbons (Figure S5).

For APC (**2**), the self-assembly patterns and the entire crystal structure are drastically altered. Two distinct HB motifs are formed (Figure 3): i) a C-H···N type HB motif is formed between the C8-H and the N3 of adjacent molecules (motif III), which connects six conformers (-**2a**-**2b**-)$_3$ alternatingly into a supermacrocyclic hexagonal barrel-like structure, barrel-1 (*vide infra*); ii) a bifurcate HB motif is formed between the phenol -OH group and the Watson-Crick edge (N1 and 6-NH_2) of adjacent molecules (motif IV), which also connects six conformers (-**2a**-**2b**-)$_3$ alternatingly into a second type of hexagonal barrel-like supermacrocyclic assembly, barrel-2 (*vide infra*) (Figure S6). Barrel-1 and -2 line up to form a continuous one dimensional host channel structure along its own C_3-axis (Figure 3).

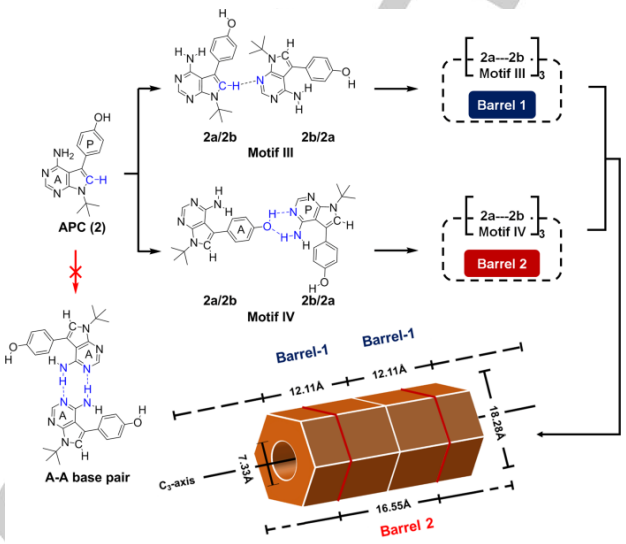

Figure 3. The HB motifs III, IV and the six-membered macrocycles, barrel-1 and barrel-2, and the schematic representation of the 1D host channel assembled by them.

According to the space-filling representations displayed in Figure 4, the top views of barrel-1 and -2 both display an equilateral hexagonal exterior (18.28 Å) and a circular interior with a diameter of 7.33 Å (Figure 3). It is worthwhile mentioning that there are solvent guest molecules located in the interior, but due to the lack of specific interactions between the host methyl groups and the guests, X-ray structural analysis cannot accurately locate the guest atoms. The PLATON/SQUEEZE tool was applied to treat these non-commensurate disordered solvent molecules. The high disorder of the solvent molecules also accounts for the higher R1 and wR values of crystal **2**, compared to **1**.

The side-views of barrel-1 and -2 are different: Barrel-1 is connected via motif III and all the individual molecular components are arranged in a fully-closed circular manner (Figure 4a); Barrel-2 is connected via motif IV and its individual molecular components are arranged in a zigzag manner, and so barrel-2 appears as a concave-convex circular structure, reminiscent of the mortise-and-tenon-joint component (Figure 4b). Thus, each individual molecule of **2** is tethered to the nearest four opposite conformational enantiomers (**2a** surrounded by four **2b**s, and *vice versa*, Figure S7) and assembles into a continuous 1D host channel structure (Figure 4c).

These 1D host channels of **2** are associated side-by-side into an overall honeycomb-like crystal structure, with one individual hexagonal channel being surrounded by six nearest channels, which are also arranged in a hexagonal manner with inter-center distance 18.64 Å (Figure 4d). The assembly of these nearby channels is longitudinally shifted along their C_3-axis in relation to the positions of the nearest barrel-1s (Figure S8). These host

10.1002/chem.201803429

channels are laterally associated through van der Waals interactions between 6-NH_2 group of one channel and one CH_3 of the *tert*-butyl group in the nearest channel (Figure S7).

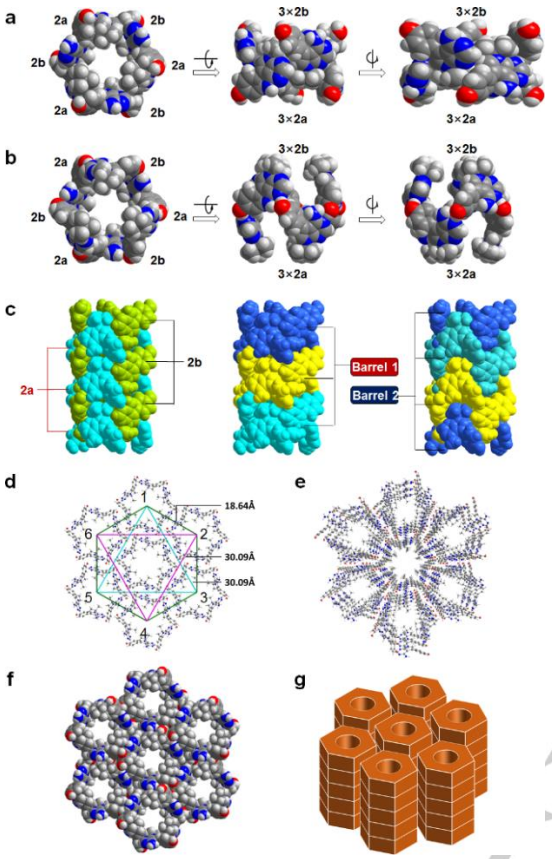

Figure 4. a,b): The space-filling top and side views of barrel-1 and barrel-2 formed by **2**. c): The side views of the 1D channel assembled by barrel-1 and barrel-2. d): The stick-ball top views of the honeycomb-like structure formed by **2**. e): The central projection of d) displaying the 1D channels. f): The top views of d) indicating the empty interiors. g): The schematic representation of the 3D honeycomb-like structure.

Next, the supramolecular assemblies of both compounds in solution were investigated. by variable temperature ^{1}H NMR (VT-NMR) [15] and ESI-MS [7b,16] techniques, two powerful methods for the examination of intermolecular interactions and species in solution state. For both **1** and **2**, according to VT-NMR, the formation of HBs between those functional groups, which participate into the HB motifs in crystal state, was confirmed in solution too (Figure S9). The DOSY-NMR measurements indicated the aggregate formation for both compounds in DMSO (Figure S10). The mass peaks of 1-mer to 4-mer of **1** and **2** in MeOH were detectable by negative mode ESI-MS. Though the molecular mass peaks of 5-mer to 6-mer of **2** were observable, their corresponding isotopic patterns were covered by noise signals due to their lower abundances (Figure S11, S12).

Since the single crystals of **1** and **2** were obtained from different solvent systems, we then analyzed their properties under the same solvent system. The morphologies of the supramolecular polymeric assemblies of **1** and **2** in solution state were revealed via SEM images. In MeOH/H_2O (10:1) system, **1** forms a membrane-covered aggregate with spherical protrusions and **2** forms a flat extending membrane aggregate (Figure S13). In the MeOH/CH_2Cl_2 (2:1) solvent system, concentration dependent morphology transitions were observed (Figure S14). At 0.5 mg/mL, **1** forms interwoven microbundles, while **2** forms a membrane structure. At 1 mg/mL, both **1** and **2** formed membrane structures. At 2 mg/mL, both compounds displayed fused vesicular morphologies, and the fusion process of individual spherical particles could be visualized by time-elapsing experiments, and some of these spherical particles contained holes, suggesting their concave interiors (Figure 5).[17] In this solvent system the spatial orientations of adjacent individual molecules in accordance with the base pair motifs I-IV, for either compound **1** or **2**, were revealed by 2D-NOESY (Figure S16).

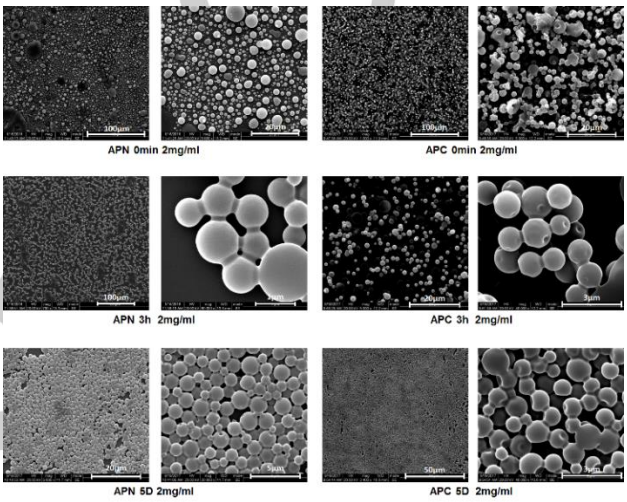

Figure 5. The supramolecular polymeric morphology formation process of APN (**1**) and APC (**2**) indicated by time-elapsing experiments at 2mg/mL within 5 days.

Upon quick evaporation of the solvents MeOH/CH_2Cl_2 (2:1), crystalline powder solids of both compounds were obtained, and they displayed distinct microcrystalline morphologies (Figure S15). To investigate their properties and inner structures, the powder samples of **1** and **2** were examined by DSC, TGA and the VT-PXRD (Figure 6). For **1**, except for the melting, the DSC experiment indicate a phase transition might happen between 115 and 135˚C (Figure 6a, Table S1), and TGA measurement indicates a sigmoid weight-loss curve (12%) within this temperature range (Figure 6b). The powder crystal of **1** displays a different PXRD spectrum from the computed spectra based on its single crystal structure at temperature range of 25 to 115˚C. Upon increasing the temperature to above 160˚C and up to 190˚C, the crystal form is then converted such that it resembles the same pattern as the computed spectrum of the single crystal of **1** (Figure 6c, S17). These findings indicate the powder solid of **1** adopts different crystal form from its single crystal obtained by the slow crystallization process mentioned above.

The lower melting point of **2** and its much smaller ΔH of the melting (9.38 kJ/mol) compared to that of **1** (27.24 kJ/mol) indicates that the crystal lattice of **2** is constructed by a weaker HB network (C-H···N type) **(**Figure 6d, Table S1**)**. The DSC and VT-PXRD experiments indicate that the powder crystalline solid of **2** adopts the same crystal form as its single crystal state at lower temperatures, and a phase transition happens at around

169˚C (Figure 6f). From the TGA measurement, a gradual linear weight loss starting from around 50˚C is found (Figure 6e), with a small inflexion between 165 and 175˚C (where a crystal phase transition happens). The gradual release of inclusion solvent molecules is due to the lack of specific interaction between the guest molecules and the host *tert*-butyl interior (which is in accordance with the findings for the single crystal state of **1**), a characteristic of non-commensurate inclusion solids.[18]

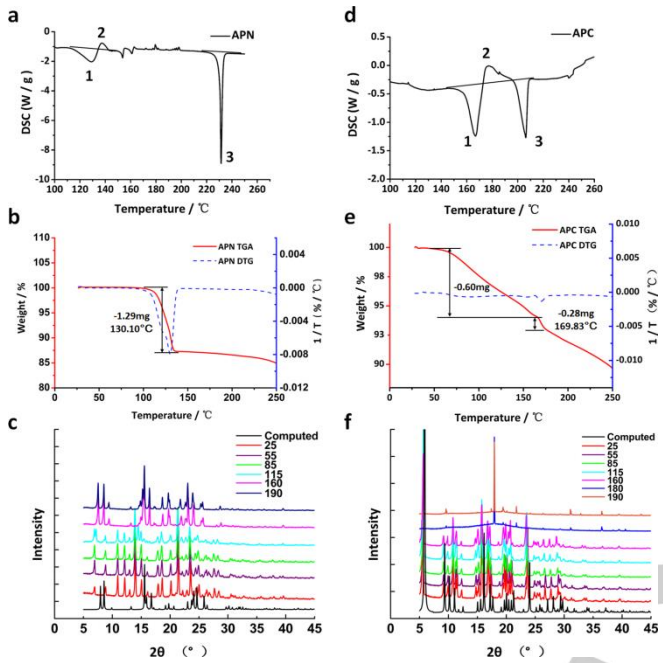

Figure 6. The DSC, TGA and VT-PXRD experiments of the powder crystalline solids of APN (**1**) and APC (**2**).

In summary, two new adenine analogues, APN (**1**) and APC (**2**), have been synthesized. Both compounds display intrinsic capabilities to form intriguing supramolecular macrocyclic structures, mediated by distinct HB base pair motifs. The conversion of nitrogen at 8 position of **1** to C8-H of **2** has a marked impact on their supramolecular structures and properties. In powder crystalline state both compounds can act as inclusion hosts, and the guest solvent molecules can be released, albeit with different release behaviours which induces phase change phenomena in both cases. These new types of adenine analogues may represent potential avenues of further development in the fields of porous or channel materials.

Experimental Section

Detailed experimental procedures and data for NMR, VT-NMR, HR-MS, X-ray, SEM and UV spectroscopy can be found in the Supporting Information.

Acknowledgements

National Natural Science Foundations of China (21572144), the Chengdu Science and Technology Program Projects (2017-CY02-00025-GX) and Testing & Analytical Center, Nuclear Magnetic Resonance Laboratory, Sichuan University are acknowledged.

Keywords: nucleobase • pyrazolo[3,4-d]pyrimidine • pyrrolo[2,3-d]pyrimidine • self-assembly • supermacrocyclic assembly

[1] a) Q. Wu, P. M. Rauscher, X. Lang, R. J. Wojtecki, J. J. de Pablo, M. J. A. Hore, S. J. Rowan, *Science* **2017**, *358*, 1434-1439; b) S. Erbas-Cakmak, D. A. Leigh, C. T. Mcternan, A. L. Nussbaumer, *Chem. Rev.* **2015**, *115*, 10081-10206; c) M. Iyoda, J. Yamakawa, M. J. Rahman, *Angew. Chem. Int. Ed.* **2011**, *50*, 10522-10553.

[2] a) B. Adhikari, X. Lin, M. Yamauchi, H. Ouchi, K. Aratsu, S. Yagai, *Chem. Commun.* **2017**, *53*, 9663-9683; b) C. Montoro-García, M. J. Mayoral, R. Chamorro, D. Gonzalez Rodriguez, *Angew Chem Int Ed Engl.* **2017**, *129*, 15855-15859; c) P. C. Ho, P. Szydlowski, J. Sinclair, P.J.W. Elder, J. Kübel, C. Gendy,L. M. Lee, H. Jenkins, J. F. Britten, D. R. Morim, I. Vargas-Baca, *Nat. Commun.* **2016**, *7*, 11299-11308; d) M. J. Hollamby, K. Aratsu, B. R. Pauw, S. E. Rogers, A. J. Smith, M. Yamauchi, X. Lin, S. Yagai, *Angew. Chem. Int. Ed.* **2016**, *55*, 9890-9893.

[3] J. L. Sessler, J. Jayawickramarajah, M. Sathiosatham, C. L. Sherman, J. S. Brodbelt, *Organic Letters* **2003**, *5*, 2627-2630.

[4] a) J. T. Davis, *Angew. Chem. Int. Ed.* **2004**, *43*, 668-698; b) J. Zhou, S. Amrane, F. Rosu, G. F. Salgado, Y. Bian, H. Tateishikarimata, E. Largy, D. N. Korkut, A. Bourdoncle, D. Miyoshi, J. Zhang, H. Ju, W. Wang, N. Sugimoto, V. Gabelica, J. L. Mergny, *J. Am. Chem. Soc.* **2017**, *139*, 7768-7779.

[5] a) M. Cai, A. L. Marlow, J. C. Fettinger, D. Fabris, T. J. Haverlock, B. A. Moyer, J. T. Davis, *Angew. Chem. Int. Ed.* **2000**, *39*, 1283-1285; b) J. T. Davis, S. Tirumala, J. R. Jenssen, E. Radler, D. Fabris, *J.Org. Chem.* **1998**, *60*, 4167-4176; c) F. Seela, T. Wiglenda, H. Rosemeyer, H. Eickmeier, H. Reuter, *Angew. Chem. Int. Ed.* **2002**, *41*, 603-605. d) D. Jiang, F. Seela, *J. Am. Chem. Soc.* **2010**, *132*, 4016-4024;

[6] J. An, R. P. Fiorella, S. J. Geib, N. L. Rosi, *J. Am. Chem. Soc.* **2009**, *131*, 8401-8403.

[7] a) A. Marsh, M. Silvestri, J. M. Lehn, *Chem. Commun.* **1996**, *13*, 1527-1528; b) H. Fenniri, P. Mathivanan, K. L. Vidale, D. M. Sherman, K. Hallenga, K. V. Wood, J. G. Stowell, *J. Am. Chem. Soc.* **2001**, *123*, 3854-3855; c) H. Fenniri, G. A. Tikhomirov, D. H. Brouwer, S. Bouatra, M. E. Bakkari, Z. Yan, J. Y. Cho, T. Yamazaki, *J. Am. Chem. Soc.* **2016**, *138*, 6115-6118.

[8] M. Mascal, N. M. Hext, R. Warmuth, M. H. Moore, J. P. Turkenburg, *Angew. Chem. Int. Ed.* **1996**, *35*, 2204–2206.

[9] a) H. Yang, M. Pan, D. Jiang, Yang He, *Org. Biomol. Chem*. **2011**, *9*, 1516-1522; b) H. Zhao, W. Huang, X. Wu, Z. Xing, Y. He, Q. Chen, *Chem. Commun.* **2012**, *48*, 6097-6099.

[10] a) M. Y. Pan, W. Hang, X. J. Zhao, H. Zhao, P. C. Deng, Z. H. Xing, Y. Qing, Y. He, *Org. Biomol. Chem.* **2011**, *9*, 5692-5702; b) H. Zhao, X. Guo, S. He, X. Zeng, X. Zhou, C. Zhang, J. Hu, X. Wu, Z. Xing, L. Chu, *Nat. Commun.* **2014**, *5*, 3108-3118.

[11] S. He, H. Zhao, X. Guo, X. Xu, X. Zhou, J. Liu, Z. Xing, L. Ye, L. Jiang, Q. Chen, Y. He, *Chem. Eur. J.* **2014**, *20*, 15473-15481.

[12] a) S. Schenone, M. Radi, F. Musumeci, C. Brullo, M. Botta, *Chem. Rev.* **2015**, *45*, 7189-7238; b) L. M. De Coen, T. S. Heugebaert, D. García, C. V. Stevens, *Chem. Rev.* **2015**, *116*, 80-139.

[13] B. Apsel, J. A. Blair, B. Gonzalez, T. M. Nazif, M. E. Feldman, B. Aizenstein, R. Hoffman, R. L. Williams, K. M. Shokat, Z. A. Knight, *Nat. chem. Biol.* **2008**, *4*, 691-699.

[14] D. E. Smith, I. Marquez, M. E. Lokensgard, A. L. Rheingold, D. A. Hecht, J. L. Gustafson, *Angew. Chem. Int. Ed.* **2015**, *54*, 11754-11759.

[15] a) A. Samanta, Z. Liu, S. K. M. Nalluri, Y. Zhang, G. C. Schatz, J. F. Stoddart, *J. Am. Chem. Soc.* **2016**, 138, 11469-11480; b) D. Samanta, I. Paul, M. Schmittel, *Chem. Commun.* **2017**, *53*, 9709-9712.

[16] K. C. Russell, E. Leize, A. V. Dorsselaer, J. M. Lehn, *Angew. Chem. Int. Ed.* **1995**, *34*, 209-213.

[17] D. M. Vriezema, J. Hoogboom, K. Velonia, K. Takazawa, P. C. M. Christianen, J. C. Maan, A. E. Rowan, R. J. M. Nolte, *Angew. Chem. Int. Ed.* **2003**, 7, 772-776.

[18] J. W. Steed, D. R. Turner, K. J. Wallace, *Core Concepts in Supramolecular Chemistry and Nanochemistry*, John Wiley & Sons, Ltd, England, **2007**, p.181.

10.1002/chem.201803429

WILEY-VCH

COMMUNICATION

Two novel adenine analogues can form either four or six-membered supermacrocyclic assemblies via distinct hydrogen bonded base pairs depending on their 8-positioned atomic identities.

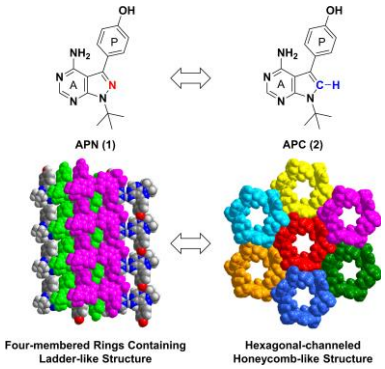

Yingying Chai, Xinglong Zhou, Changfu Li, Beibei Ma, Zhen Shen, Ridong Huang, Hai Chen, Bojiang Chen, Weimin Li and Yang He**

Page No. – Page No.

Supermacrocyclic assemblies by Hydrogen-Bond Codes of C7-Phenol Pyrazolo and Pyrrolo Derivatives of Adenine